Bioorganic & Medicinal Chemistry Letters 20 (2010) 1272–1277

Contents lists available at ScienceDirect

Bioorganic & Medicinal Chemistry Letters

journal homepage: www.elsevier.com/locate/bmcl

Oxime Carbamate—Discovery of a series of novel FAAH inhibitors

S. Y. Sit [a,*], Charles M. Conway [b], Kai Xie [a], Robert Bertekap [b], Clotilde Bourin [b], Kevin D. Burris [a,b,†]

[a] Department of Chemistry, Bristol-Myers Squibb Research & Development, 5 Research Parkway, Wallingford, CT 06492-7660, USA
[b] Neuroscience Drug Discovery, Bristol-Myers Squibb Research & Development, 5 Research Parkway, Wallingford, CT 06492-7660, USA

ARTICLE INFO

Article history:
Received 12 November 2009
Accepted 17 November 2009
Available online 24 November 2009

Keywords:
Oxime
Carbamate
FAAH
Inhibitor
Fatty acid amide hydrolase
Endocannabinoid
Molecular modeling
Inhibition kinetic
Signaling lipid
Cannabinoid
Anandamide
Antiinflammatory
Signal termination
Marijuana
Nociception
Pain
Tetrahydrocannabinol
Antinociceptive
Electrophilic recognition
Urea
Bisarylazole carbamates
Preclinical model
Nonprostanoid
Prostacyclin
Cholesterol
Eicosanoid
Isoprenoid
Essential fatty acid
Curtius
para-Phenoxy
Biphenyl
Reversible
Hammond's Postulate
Hargreaves
1MT5
2VYA

ABSTRACT

A series of novel oxime carbamates have been identified as potent inhibitors of the key regulatory enzyme of the endocannabinoid signaling system, fatty acid amide hydrolase (FAAH). In this Letter, the rationale behind the discovery and the biological evaluations of this novel class of FAAH inhibitors are presented. Both in vitro and in vivo results of selected targets are discussed, along with inhibition kinetics and molecular modeling studies.[1]

FAAH is an integral membrane hydrolase with a single N-terminal transmembrane domain. It is responsible for the hydrolytic cleavage of a variety of membrane-bound signaling lipid substances, including members of the endogenous cannabinoids (endocannabinoids) such as *N*-arachidonoylethanolamine (anandamide) and, the

* Corresponding author.
E-mail address: sits@bms.com (S.Y. Sit).
† Present address: Lilly Research Laboratories Bldg 48, Floor 3, D/C 0536 Lilly Corporate Center Indianapolis, IN 46285, USA.

0960-894X/$ - see front matter © 2009 Elsevier Ltd. All rights reserved.
doi:10.1016/j.bmcl.2009.11.080

anti inflammatory factor *N*-palmitoyl ethanolamine (PEA). In mammals, many biological signaling circuitries are directly and indirectly regulated by small lipid molecules, the signal termination step is thus achieved by the degradation of these lipids by enzymes such as FAAH.

Cannabinoid receptors are widely distributed, both centrally and peripherally. Human experiences with marijuana from different cultures; and the on-going desire to selectively harness the beneficial effects of marijuana, have transformed endocannabinoid research into a well-developed field. Our interest in the area stems from the notion that the specific biological effects triggered by the local activation of the central cannabinoid type 1 (CB1) receptors could modulate nociception, in contrast to the indiscriminate, global activation by an exogenous cannabinoid such as tetrahydrocannabinol (Δ^9-THC). Many inhibitors of the FAAH have been demonstrated to elicit antinociceptive effects in standard animal models of pain. However, it is of special importance to determine if the desired antinociceptive effects resulting from stimulation of endocannabinoid activity can be separated from the unwanted sedative/ataxic actions.

A brief survey of recently published inhibitors of FAAH revealed many carbamate-containing compounds, a structural class that has been grouped into a generic class by recent reviewers.[2] Along with the analogous urea-containing inhibitors, it is generally supposed that the carbonyl functional group acts as the electrophilic recognition site. In a few instances, the actual carbamoylated intermediates were identified by mass spectroscopy,[3a] and in several recent papers the actual carbamoylated FAAH proteins were isolated and its crystal structure determined.[3b,3c]

We recently disclosed a series of bisarylazole carbamates as inhibitors of FAAH that demonstrated potent analgesic properties in a battery of standard in vivo preclinical models of pain.[4] While very potent and promising, the bulky bisarylazole chemotype lacks physicochemical properties desirable for efficient uptake and distribution in vivo. The original bisaryl substituted imidazole core has appeared in a number of nonprostanoid prostacyclin mimetics; hypo-cholesterolemic agents and antiinflammatory agents targeted at various biological cascades closely related to prostacyclin, cholesterol, and eicosanoid biosyntheses.[5a–c] These, in turn, have the semblance of the cellular metabolic pathways of the isoprenoid, arachidonic acid, and related essential fatty acids (EFA), This thought led us to investigate the possibility of replacing the bisarylazole moiety with other simple lipophilic groups, especially simple long hydrocarbon chains. Using the bisarylazole as a starting template, we hypothesized that the bulky lipophilic end of the molecule **1** could possibly be truncated in size while keeping the crucial carbamate moiety intact. At first we utilized the classical biphenyl ethers **2** and simple biphenyl **3** groups to mimic the original bulky bisarylazole moiety (Fig. 1).

Both compounds **2** and **3** showed some FAAH activity, but were substantially less active than the original diphenyl substituted imidazole parent compound **1**. We speculated that these aromatic derivatives are rather rigid,[6] they do not present themselves in low energy conformations that fit into the lipophilic pocket that recognizes the lipophilic tail group in **1**.

Our synthetic chemistry effort thus expanded to include additional lipophilic 'tail groups' such as simple aliphatic chains. Schemes 1 and 2 shown here briefly summarize the syntheses of the target compounds and their intermediates. In general, all the carbamate targets in the present study were prepared by acylation of the isocyanates with oximes. The isocyanate intermediates were conveniently prepared by Curtius rearrangement of the corresponding carboxylic acids, while oximes were made directly from aldehydes.[7]

In order to introduce a limited degree of conformational freedom, we replaced the *para*-phenoxy ring in **2**, by simple alkoxy

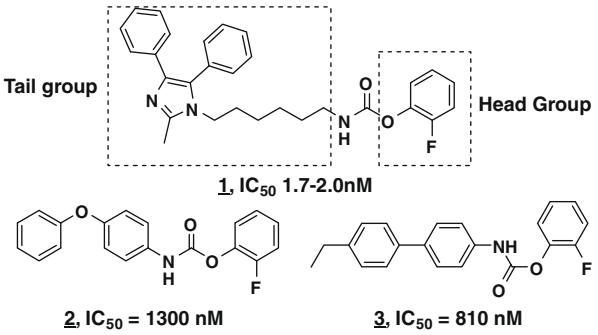

Figure 1. Initial attempts using simple biphenyl ether **2**, and *para*-substituted biphenyl **3** to mimic the lipophilic tail end of **1**.

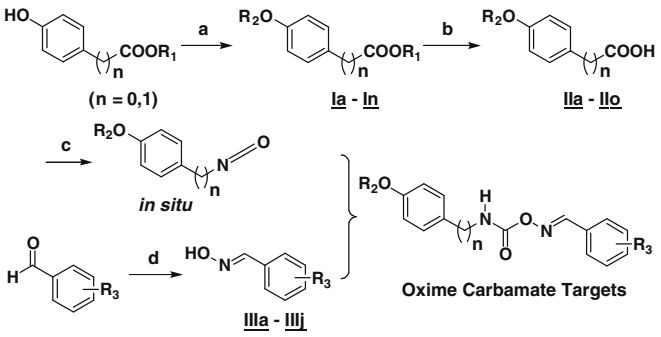

Scheme 1. General reactions and conditions: (a) alkyl bromide, NaH, DMF at rt; (b) NaOH then H^+; (c) Et_3N, DPPA, toluene rt→105 °C, then oxime IIIa–IIIj; (d) $H_2NOH{\cdot}HCl$, K_2CO_3 in EtOH at rt.

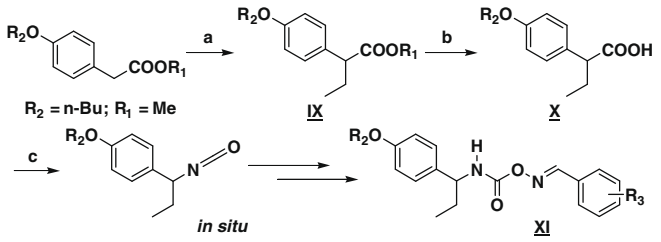

Scheme 2. General reactions and conditions: (a) EtBr, NaH, DMF at 50 °C; (b) NaOH then H^+; (c) Et_3N, DPPA, toluene rt→105 °C, then oxime components.

chains, to give target compounds **4**–**9** (Fig. 2). The original intention was to use the alkoxy chain to mimic, and to maximize the lipophilic contacts, as in the parent bisarylazole prototype.

The initial set of targets (Fig. 2) were shown to have IC_{50} values ranging from 340 nM to 8 nM, with the activity spectrum spread favorably toward having a longer alkoxy chain attached to the aniline end of the carbamate core. The most active compound, **7** from the series is unique due to an additional carbon spacer inserted, hence separating the carbamate nitrogen from the aniline ring. Next we focused on the series that had a methylene spacer between the carbamate nitrogen and the phenyl ring. Introducing a spacer did indeed produce active compounds that were only comparable to **7** (Supplementary data). However, no substantial improvement in inhibitory potency was observed with the methylene spacer. It appeared that the insertion of a methylene link, and thus the change in pK_a of the carbamate nitrogen, did not have any significant impact toward FAAH inhibition.

Visual inspection of the molecular structure of the MAP (methoxyarachidonyl phosphonate) bound FAAH protein crystal 1MT5 obtained from the Protein Data Bank (PDB) showed a very well

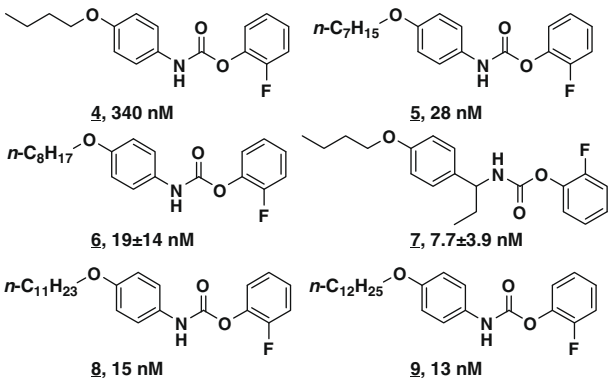

Figure 2. Replacing the terminal phenyl ring in **2** with simple hydrocarbon chain greatly improves FAAH inhibitory activities. Data given in IC_{50} ± SEM nM whenever available.

defined lipophilic channel network that is surrounded by mostly nonpolar, lipophilic amino acid side chains. Only a portion of the lipophilic channel (the 'acyl-binding', AB channel) is occupied by the covalently bound MAP ligand while the remaining channel space appear to be unoccupied.[8] It has been suggested that the other channel that branches out from that occupied by the MAP ligand, could serve as the access passage (the 'membrane-access', MA channel) for the byproducts from the enzymatic hydrolysis process.

Upon further examination of 1MT5 also revealed an additional lipophilic pocket, positioned somewhat along the forward projection of the OCH_3 in the original MAP ligand, and that region is partly defined by **Met191**-**Phe192**-**Cys269**-**Val270**-**Tyr271**-**Leu278**. Our intuitions suggested that it would be highly desirable if the carbamate oxygen end is lengthened by 1–2 atoms, thus extending the head group into that lipophilic region. This idea led us to a series of oxime carbamates that incorporated an alkoxy aniline chain and a simple acetoxime head group, as summarized in Figure 3.

It is clear from these results that SAR for FAAH inhibition strongly favors the longer chains that could possibly mimic the original arachidonyl chain. The optimum activity in the acetoxime series appeared to peak at chain lengths of C_8–C_{10} carbon atoms. The optimal length is likely to be independent of the oxime head group if the hydrocarbon chain is to reside within the lipophilic channel and if that is indeed its preferred orientation. This chain length dependence was confirmed in several other series of analogs with different oxime cores. In all cases, the optimum chain lengths peaked at C_8–C_{11}, as summarized in Figure 4.[9]

A qualitative molecular modeling study using 1MT5 as the input structure on Schrodinger 2008's 'Maestro Suite, Version 8.5. Schrödinger, LLC, New York, NY, 2008' was carried out in an effort to try to understand the role that the oxime carbamate functional group plays in FAAH recognition.[10]

Docking experiments on a set of C_1–C_{14} oxime carbamates were performed in such a way that the inhibitor was allowed to move about freely while a distance constraint was imposed upon the carbamate carbonyl oxygen atom so that it was within a sphere of 1.0 Å radius, as defined by the coordinates of the oxygen atom of the phosphonate group in the 'modified' FAAH–MAP structure.[10a] The longest chain, 14 carbons, failed at times to return any low energy complementary pairs, presumably due to the limited channel length. Chain lengths of 4–13 carbon atoms long consistently yielded high scores while shorter chains could fit into the lipophilic channel in multiple orientations with lower scores.[11] Amongst the highest scored structures, an additional hydrogen-bond (HB) is clearly present between the carbamate NH and **Met191** (average ~2.1 Å).[12] It is suspected that the HB might very well be real and that could contribute, at least in part, to the high observed inhibitory activities associated with these oxime carbamates. More recently, an additional FAAH crystal structure (2VYA) became available on a 'humanized' rat (*h/r*) FAAH, covalently bound to the partial ligand PF-750 (leaving group no longer visible) through **Ser241** linked carbamate linkage.[3b] The crystal structures 1MT5 and 2VYA are remarkably similar with their complete backbones (~540 residues) superimposed onto each other to less than 0.43 Å RMSD. However some subtle differences were clearly visible once all the side chain attachments were compared. As it was pointed out in the original paper that perhaps the most striking difference is the relative orientation of **Phe432**, in 2VYA, that can 'flip' out of the cystolic membrane access channel thus effectively enlarging the channel access opening. The driving force behind this conformational change is uncertain. Perhaps the smaller, bound molecular dimension of PF-750 is partly responsible for such conformational switch-over. Furthermore, it is unknown which of the orientations represents the resting state, or if the existence of one conformation is driven by the presence of a particular ligand. It is interesting to point out that once the side chain of **Phe432** is within the 'AB' pocket, as in the case of 2VYA, the AB channel space is expected to be substantially reduced, and would no longer accommodate long chain inhibitors like ours. Our hypothesis of oxime carbamate ligand fitness with respect to the reduction in AB channel length is tested using a similar grid model generated from the

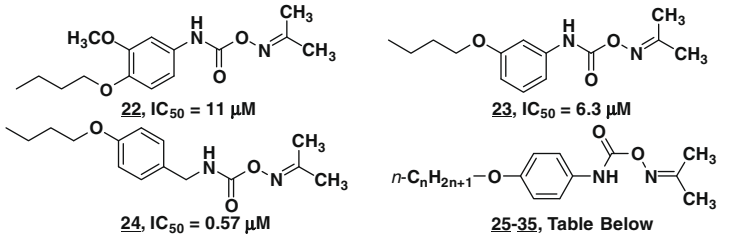

compound #	n	IC_{50}/nM	compound #	n	IC_{50}/nM
25	2	730	**31**	8	2.4±1.9
26	3	210±56	**32**	9	2.1±1.6
27	4	28±1.0	**33**	10	2.2
28	5	28±9.0	**34**	11	4.9
29	6	18	**35**	12	5.0
30	7	8.4±1.3			

Figure 3. Oxime carbamate group showed greatly enhanced FAAH activity over simple carbamates. Activity is mainly a function of the alkyloxy chain length. Data from average 2–5 replicates.

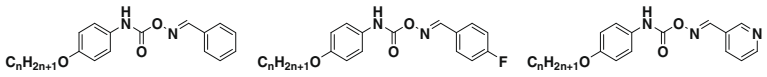

n	#	IC_{50}/nM	n	#	IC_{50}/nM	n	#	IC_{50}/nM
1	**36**	290	NA		NA	NA		NA
2	**37**	81±17	2	**48**	46±19	2	**59**	150±34
3	**38**	9.3±4.0	3	**49**	13±2	3	**60**	29±6
4	**39**	8.5±2.3	4	**50**	2.2±0.9	4	**61**	14±5
5	**40**	3.5±0.7	5	**51**	1.8±0.4	5	**62**	6.1±1.0
6	**41**	8.0±0.8	6	**52**	6.5±4.2	6	**63**	8.3±0.8
7	**42**	8.6±5.9	7	**53**	2.3±1.8	7	**64**	2.3±0.7
8	**43**	0.43±0.15	8	**54**	0.27±0.06	8	**65**	0.8±0.3
9	**44**	0.25±0.07	9	**55**	0.2	9	**66**	0.65±0.49
10	**45**	0.35±0.07	10	**56**	0.25±0.07	10	**67**	0.35±0.07
11	**46**	0.45±0.07	11	**57**	0.40	11	**68**	0.15±0.07
12	**47**	2.4	12	**58**	2.1	12	**69**	0.35±0.07

Figure 4. Results with similar trends were reproduced in analogous systems. IC_{50} values given in nM from average 2–5 replicates, NA stands for data not available.

crystal structure of 2VYA but was fitted with the oxime carbamate ligands from Figure 4.[10a]

Indeed most of the longer chain ($n \geqslant 6$) analogs fitted poorly while shorter chain (n <6) oxime carbamates docked in multiple ligand orientations, also with poorer scores. The docking process also resulted in a few false high scored ligand conformations for the longer chain candidates (n = 7–10) but those unlikely conformations were rejected because they could only be fitted either with a substantial displacement of the carbamate carbonyl moiety from the oxyanion hole; or by forcing the longer hydrocarbon chain to reside within a narrow passage away from the space surrounded by **Phe432** and **Met436-Trp531**. Interestingly, it was observed from the modeling study that both unfavorable scenarios for the longer chain ligands (n = 7–12), could be avoided entirely by simply flipping the **Phe432** residue *very slightly* to open up the acyl-chain binding channel to nearly its full length (Fig. 5).

In fact we have long been puzzled by the empirical relationship that the IC_{50} values that showed a distinct 'dip' at chain lengths 6–7 before it goes up again (Data from Fig. 4), and peak at 9–11 before it comes down in all three series of analogs (Fig. 6). Taken together, our results suggested that a dynamic change in **Phe432** conformation is possibly behind this observation.

One of the more active compounds, **50**, with a shorter C_4 alkyl chain and an IC_{50} = 2.2 nM, was chosen for testing in whole animal pain models—Hargreaves thermal escape test, as described previously.[4,13] Although not the most active compound generated from the present study, the shorter C_4 chain analog gave us a broader possibility of options for dosing in vivo.

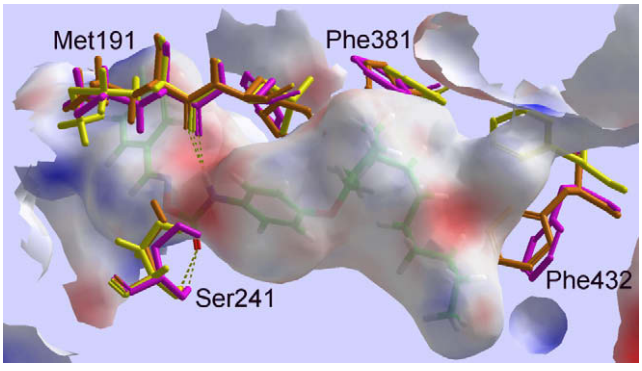

Figure 5. Docking of one of the C_{12} alkoxyphenyl oxime carbamates **58** (shown in green) on a grid model generated from the crystal structure of 2VYA, with the phenyl oxime head group of **58** pointing away from the LHS of the viewer. The best scorers require that the longer chain ligands to occupy a portion of the 'AB' channel. Shown here with the **Phe432** of 2VYA displaced slightly (magenta) to accommodate the full length of **58**. The original crystal structure of 1MT5 is shown in yellow, and 2VYA in brown.

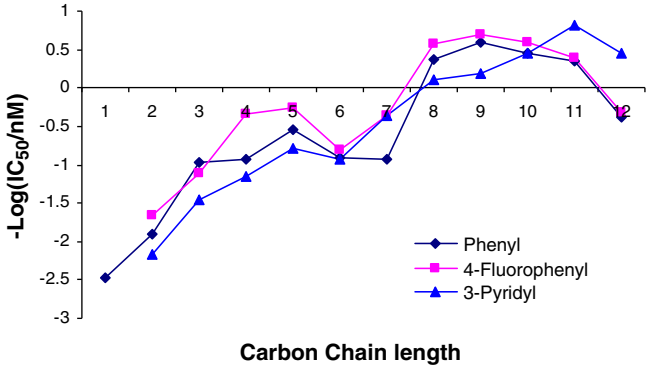

Figure 6. Plot of $-\log_{10}$(Numerical IC_{50} values) from Figure 4 against carbon chain length on all three series of data. A characteristic 'dip' in activity is clearly visible at chain lengths 6–7 in all three series.

All rats received two intravenous injections (−15 min, 0 min) with vehicle treatment (CEW + CEW) and morphine (3 mg/kg, iv; 0 min) acting as negative and positive controls, respectively. Compound **50** (0.1, 1, and 10 mg/kg, iv) given 15 min prior to exogenous anandamide (1 mg/kg, iv) produced a dose-dependent antinociceptive effect that differed significantly from vehicle-treated controls throughout the 32 min test for the two higher doses (Fig. 7). Neither 1 mg/kg anandamide nor 10 mg/kg of compound **50** was active if given alone, but together their effect was comparable to the positive control morphine sulfate (3 mg/kg, iv). Compound **50** transformed the inactive dose of anandamide generating a robust antinociceptive effect only seen with higher doses of exogenous anandamide (e.g., 5–15 mg/kg, iv). Given that FAAH is responsible for the hydrolytic cleavage of anandamide, the demonstrated potentiation of exogenous anandamide by compound **50** (where combination of two inactive doses yielding a robust antinociceptive effect) is consistent with the actions of an inhibitor of FAAH and provides in vivo proof of concept for the mechanism. Importantly, this antinociceptive action was observed without strong sedation or akinesia providing evidence for the ability to separate the desirable antinociceptive actions of FAAH inhibition from the unwanted adverse effects.

One constantly recurring question is that the carbonyl group is believed to act as the electrophilic center for irreversible inhibition. Indeed, Cravatt et al. has demonstrated the covalent binding of

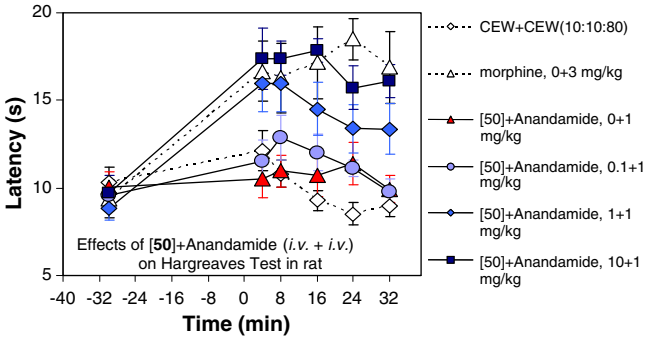

Figure 7. Compound **50** (0.1, 1 & 10 mg/kg, iv; −15 min) potentiated the antinociceptive effects (but not the sedative effects) of an inactive dose of exogenous anandamide (1 mg/kg, iv; 0 min) showing a peak effect comparable to morphine (3 mg/kg, iv; 0 min). Vehicle CEW stands for cremophor/ethanol/water.

PF-750,[3b,3c] by isolating the inhibitor-modified FAAH protein. Using a 'humanized rat' (*h/r*) FAAH protein, they were able to determine the 3-dimensional structures of the inhibitor-bound FAAH. In another recent paper,[3d] the same group described the binding and inactivation mechanism of a *h/r* FAAH by α-ketoheterocycle inhibitors. In that study the actual structure of the protein bound deprotonated hemiketal of the reversible, α-ketooxazole inhibitor, OL-135 is revealed by X-ray crystallography. Without doubt, the structures of these inhibitor-bound FAAH proteins allowed the researchers to scrutinize, most likely, the final phase of the inhibition process, it is uncertain if the key biological event (i.e., enzyme inhibition) occurred on the same chemical kinetic time scale. In other words, the observation of a covalently bound protein could represent simply a recognition process downstream from the enzyme inactivation. The classical mechanistic interpretation suggests that if the lower energy transition state of the receptor–inhibitor complex lies toward the product side, the forward process would be likely to occur, that is, formation of covalent binding. Conversely if the lower energy transition state occurs prior to the activation barrier, the initial ligand–protein complex will likely dissociate back without forming any covalent bond.[14] We therefore designed a series of kinetic studies to probe the inhibitory kinetics of these oxime carbamate analogs.

Firstly, standard substrate–velocity plots (Fig. 8) show no change in V_{max} while apparent K_m increases with increasing inhibitor, suggesting compound **50** is a competitive inhibitor (K_i ~30 nM).[15] Secondly, the reversibility of inhibition was demonstrated by wash-out

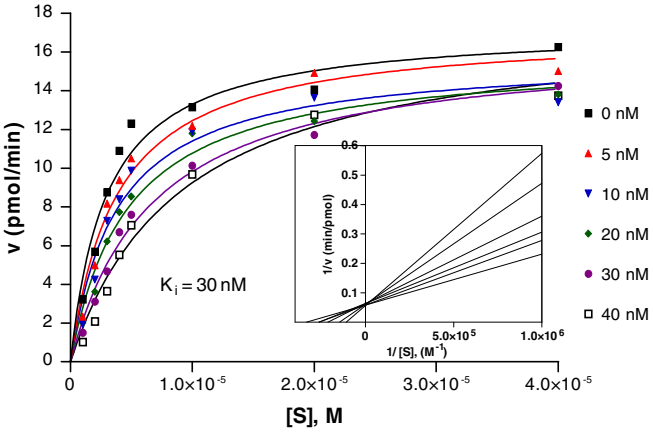

Figure 8. Competitive inhibition of FAAH by compound **50** at multiple concentrations of inhibitor. The inset double reciprocal plot (derived from the K_m and V_{max} values calculated from non-linear regression of the substrate–velocity curves) shows the characteristic constant V_{max} of a competitive inhibitor.

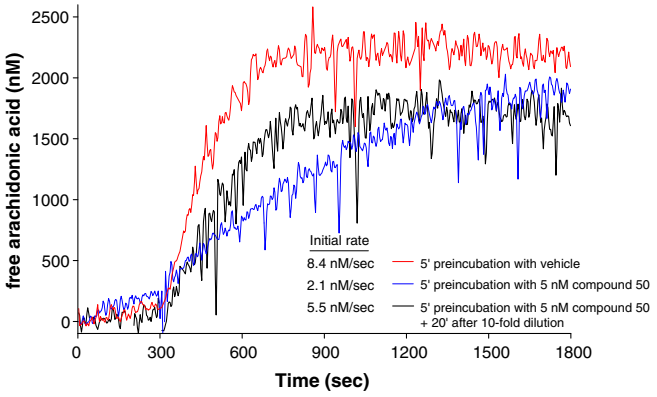

Figure 9. The release of arachidonic acid by FAAH mediated hydrolysis of anandamide in the presence of compound **50** was measured over time. Note the inhibition of the reaction with 5 nM compound **50** (blue trace) relative to vehicle treatment (red trace). Upon 10× dilution of the inhibitor, FAAH activity was partially restored (black trace).

experiments. In a fluorescent assay measuring the production of arachidonic acid in real time, 5 nM compound **50** reduced the initial FAAH reaction rate to 25% of vehicle treated enzyme. 10-fold dilution of the inhibitor resulted in a nearly threefold increase in initial reaction rate (to 65% of vehicle), demonstrating dissociation of the initial inhibitor–FAAH complex back to the *active* FAAH (Fig. 9).[16] Additional washout experiments utilizing repeated centrifugation to effect more thorough removal of the inhibitor demonstrated complete recovery of FAAH activity (see Supplementary data).

In conclusion the oxime carbamate moiety is a novel design element for the construction of novel carbamate bearing FAAH inhibitors. Potent enzyme inhibition, together with demonstrated in vivo activity could be achieved with a linear alkoxy chain attached to a phenyl ring, designed to mimic the arachidonyl chain found in the natural substrate. Molecular modeling suggested that hydrogen bond formation of the carbamate NH with **Met191** is within reach. Docking experiments also suggested that a dynamic conformational flipping of **Phe432** is possibly driven by the shape and size of the ligand. The additional HB formation, together with the proximal carbonyl recognition site interactions, adjacent to the largely hydrophobic channel could firmly anchor the oxime carbamate ligand in the AB channel. Furthermore, kinetic studies confirmed the competitive and reversible nature of inhibition of the oxime carbamate derivatives.

Supplementary data

Supplementary data associated with this article can be found, in the online version, at doi:10.1016/j.bmcl.2009.11.080.

References and notes

1. A preliminary report of this work was recently presented. Sit, S. Y.; Conway, C.; Xie, K.; Bertekap, R.; Bourin, C.; Burris, K. and Deng, H. Poster Abstracts # 106, 31st National Medicinal Chemistry Symposium, Pittsburgh PA, Jun 15, 2008–Jun 19, 2008.
2. General review of the state of the art: Seierstad, M.; Breitenbucher, J. G. *J. Med. Chem.* **2008**, *51*, 7327.
3. (a) Alexander, J. P.; Cravatt, B. F. *Chem. Biol.* **2005**, *12*, 1179; (b) Mileni, M.; Johnson, D. S.; Wang, Z.; Everdeen, D. S.; Liimatta, M.; Pabst, B.; Bhattacharya, K.; Nugent, R. A.; Kamtekar, S.; Cravatt, B. F.; Ahn, K.; Stevens, R. C. *Proc. Natl. Acad. Sci. U.S.A.* **2008**, *105*, 12820; Additional crystal structure—2WAP has very recently emerged: (c) Ahn, K.; Johnson, D. S.; Mileni, M.; Beidler, D.; Long, J. Z.; McKinney, M. K.; Weerapana, E.; Sadagopan, N.; Liimatta, M.; Smith, S. E.; Lazerwith, S.; Stiff, C.; Kamtekar, S.; Bhattacharya, K.; Zhang, Y.; Swaney, S.; Van Becelaere, K.; Stevens, R. C.; Cravatt, B. F. *Chem. Biol.* **2009**, *16*, 411; There are two newly released, FAAH crystal structures—2WJ1 and 2WJ2 are subjects of: (d) Mileni, M.; Garfunkle, J.; DeMartino, J. K.; Cravatt, B. F.; Boger, D. L.; Stevens, R. C. *J. Am. Chem. Soc.* **2009**, *131*, 10497.

4. Sit, S. Y.; Conway, C.; Bertekap, R.; Xie, K.; Bourin, C.; Burris, K.; Deng, H. *Bioorg. Med. Chem. Lett.* **2007**, *17*, 3287.
5. (a) Meanwell, N. A.; Rosenfeld, M. J.; Wright, J. J. K.; Brassard, C. L.; Buchanan, J. O.; Federici, M. E.; Fleming, J. S.; Gamberdella, M.; Hartl, K. S.; Zavoico, G. B.; Seiler, S. M. *J. Med. Chem.* **1993**, *36*, 3871; (b) Seiler, S. M.; Brassard, C. L.; Federici, M. E.; Romine, J.; Meanwell, N. A. *Prostaglandins* **1997**, *53*, 21; (c). *J. Med. Chem.* **1994**, *37*, 560; (d) Magnin, D. R.; Biller, S. A.; Wetterau, J.; Robl, J. A.; Dickson, J. K.; Taunk, P.; Harrity, T. W.; Lawrence, R. M.; Sun, C.-Q.; Wang, T.; Logan, J.; Fryszman, O.; Connolly, F.; Jolibois, K.; Kunselman, L. *Bioorg. Med. Chem. Lett.* **2003**, *13*, 1337; (e) Sharpe, T. R.; Cherkofsky, S. C.; Hewes, W. E.; Smith, D. H.; Gregory, W. A.; Haber, S. B.; Leadbetter, M. R.; Whitney, J. G. *J. Med. Chem.* **1985**, *28*, 1188; (f) Kahlon, D. K.; Lansdell, T. A.; Fisk, J. S.; Hupp, C. D.; Friebe, T. L.; Hovde, S.; Jones, A. D.; Dyer, R. D.; Henry, R. W.; Tepe, J. J. *J. Med. Chem.* **2009**, *52*, 1302.
6. Previous results obtained by others showed that *meta*-oriented biphenyls and phenoxyphenyls analogs on a different core demonstrated potent FAAH inhibitors: (a) Mor, M.; Lodola, A.; Rivara, S.; Vacondio, F.; Duranti, A.; Tontini, A.; Sanchini, S.; Piersanti, G.; Clapper, J. R.; King, A. R.; Tarzia, G.; Piomelli, D. *J. Med. Chem.* **2008**, *51*, 3487; (b) Mor, M.; Rivara, S.; Lodola, A.; Plazzi, P. V.; Tarzia, G.; Duranti, A.; Tontini, A.; Piersanti, G.; Kathuria, S.; Piomelli, D. *J. Med. Chem.* **2004**, *47*, 4998; (c) Tarzia, G.; Duranti, A.; Gatti, G.; Piersanti, G.; Tontini, A.; Rivara, S.; Lodola, A.; Plazzi, P. V.; Mor, M.; Kathuria, S.; Piomelli, D. *Chem. Med. Chem.* **2006**, *1*, 130.
7. Sit, S. Y.; Xie, K.; Deng, H. (Bristol-Myers Squibb Co., USA), (Oxime)carbamoyl fatty acid amide hydrolase inhibitors, US Patent 6,949,574, September 25, 2005.
8. Bracey, M.; Hanson, M. A.; Masuda, K. R.; Stevens, R. C.; Cravatt, B. F. *Science* **2002**, *298*, 1793; McKinney, M. K.; Cravatt, B. F. *Annu. Rev. Biochem.* **2005**, *74*, 411.
9. For comparison purposes, a subset of selected 'simple carbamate' analogs were screened, and results can be found in the Supplementary data.
10. a The crystal structure of 1MT5 has been used by many researchers in the field. The exact technique used to generate useful information varies from group to group. For example: methods for modeling study can be found in the Supplementary data to Ref. 10.; (b) Guimarães, C. R. W.; Boger, D. L.; Jorgensen, W. L. *J. Am. Chem. Soc.* **2005**, *127*, 17377; (c) Boger, D. L.; Miyauchi, H.; Du, W.; Hardouin, C.; Fecik, R. A.; Cheng, H.; Hwang, I.; Hedrick, M. P.; Leung, D.; Acevedo, O.; Guimaraes, C. R. W.; Jorgensen, W. L.; Cravatt, B. F. *J. Med. Chem.* **2005**, *48*, 1849; (d) Keith, J. M.; Apodaca, R.; Xiao, W.; Seierstad, M.; Pattabiraman, K.; Wu, J.; Webb, M.; Karbarz, M. J.; Brown, S.; Wilson, S.; Scott, B.; Tham, C.-S.; Luo, L.; Palmer, J.; Wennerholm, M.; Chaplan, S.; Breitenbucher, J. G. *Bioorg. Med. Chem. Lett.* **2008**, *18*, 4838.
11. Docking with multiple ligand orientations has been reported, for instance Ref. 10b.
12. **Met191** hydrogen bond formation with carbamate NH has been implicated in FAAH inhibition: Saario, Ref. 10b; and more recently in: Saario, S. M.; Poso, A.; Juvonen, R. O.; Jaervinen, T.; Salo-Ahen, O. M. H. *J. Med. Chem.* **2006**, *49*, 4650.
13. (a) Dirig, D. M.; Salami, A.; Rathbun, M. L.; Ozaki, G. T.; Yaksh, T. L. *J. Neurosci. Methods* **1997**, *76*, 183; (b) Hargreaves, K.; Dubner, R.; Brown, F.; Flores, C.; Joris, J. *Pain* **1988**, *32*, 77.
14. Given the observed reversible inhibition, the statement is a form of the Hammond's Postulate. Hence whatever carbonyl interactions oxime carbamate might have such as those with **Ser241**, the hydroxy oxygen atom is not close enough to get past the energy barrier to establish a covalent bond.
15. The K_m and V_{max} for each substrate–velocity curve was calculated through non-linear regression of the Michaelis–Menten equation, $v = (V^*_{max}[S])/(K_m + [S])$, using GraphPad Prism, with $R^2 \geqslant 0.94$ for all curves. The inset plot of the double-reciprocal (Lineweaver–Burke) plot was created by constructing and plotting each line using the calculated K_m and V_{max} values from the non-linear regression and was produced to visually show the constant V_{max} values with increasing inhibitor concentration.
16. H4 cells that express transfected human FAAH were used for all in vitro experiments. See Ref. 4 for details.